

# Formation of Transparent Conducting Films Based on Core-Shell Latices: Influence of the Polypyrrole Shell Thickness

F. M. HUIJS,<sup>1,2</sup> J. LANG,<sup>3</sup> D. KALICHARAN,<sup>4</sup> F. F. VERCAUTEREN,<sup>2</sup> J. J. L. VAN DER WANT,<sup>4</sup> G. HADZIOANNOU<sup>1</sup>

<sup>1</sup> Department of Polymer Chemistry, Materials Science Centre, University of Groningen, Nijenborgh 4, 9747 AG Groningen, The Netherlands

<sup>2</sup> TNO Institute of Industrial Technology, Division of Materials Technology, P.O. Box 6235, 5600 HE Eindhoven, The Netherlands

<sup>3</sup> Institut Charles Sadron, CNRS-ULP Strasbourg, 6 rue Boussingault, 67083 Strasbourg Cedex, France

<sup>4</sup> Laboratory for Cell Biology and Electron Microscopy, University of Groningen, Oostersingel 69-11, 9713 EZ Groningen, The Netherlands

*Received 8 November 1999; accepted 31 March 2000*

**ABSTRACT:** Transparent conducting latex films have been prepared from core-shell latices. The latex particles have a poly(butyl methacrylate) (PBMA) core of about 700 nm and a very thin polypyrrole (PPy) shell. We have studied the film formation of latices with 1, 2, and 4 wt % PPy and compared this with the film formation of the pure PBMA latex. The film formation process was studied by transparency measurements, atomic force microscopy surface flattening, and transmission electron microscopy on ultrathin sections of films after various annealing times at 120°C. It is demonstrated that highly transparent (>90%) and antistatic films can be produced using these latices. The presence of a polypyrrole shell around the PBMA latex particle seriously hinders the deformation of the particles. The amount of polypyrrole, and thus the shell thickness, is the determining factor for the speed of film formation. © 2000 John Wiley & Sons, Inc. *J Appl Polym Sci* 79: 900–909, 2001

**Key words:** film formation; core-shell latex; transparent; antistatic; polypyrrole

## INTRODUCTION

Intrinsically conductive polymers (ICPs) are widely studied because of their many potential applications. Polypyrrole (PPy) is one of the most investigated among the ICPs because of its relatively air-stable conductivity. Good air-stability is

one of the important demands for the practical use of these materials (e.g., as an antistatic coating). For such applications a resistance in the range between  $10^5$  and  $10^8 \Omega/\square$  is needed, a range well feasible with ICPs. One of the major drawbacks of ICPs, however, is the still limited processability of these polymers. Usually ICPs are not soluble in common solvents. Polyaniline (PANI) protonated with selected sulfonic esters or phosphoric acid diesters is soluble in solvents like *N*-methylpyrrolidone (NMP),<sup>1</sup> *m*-cresol,<sup>2</sup> and in selected fluorinated alcohols.<sup>3</sup> Solutions of PANI have also been prepared in strong acids like pyru-

*Correspondence to:* G. Hadziioannou (hadzii@chem.rug.nl).  
Contract grant sponsor: Senter IOP Surface Technology;  
contract grant number: IOT 95001 B.

*Journal of Applied Polymer Science*, Vol. 79, 900–909 (2001)  
© 2000 John Wiley & Sons, Inc.

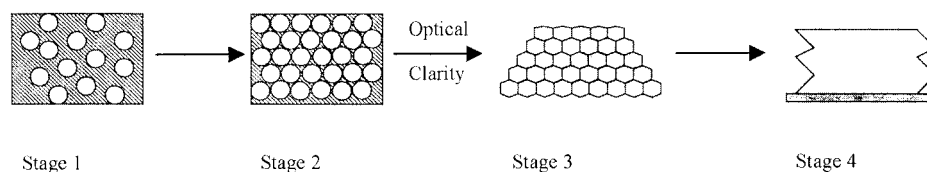


**Figure 1** Schematic presentation of the four stages of aqueous latex film formation.

vic acid<sup>4</sup> or concentrated sulfuric and other strong acids.<sup>5,6</sup> Lee et al.<sup>7</sup> have synthesized conducting polypyrrole solutions in organic solvents like *m*-cresol; however, because of safety and environmental regulations, there is a need for water-based processable ICPs. Bayer AG has developed a water-based processable polythiophene, poly(3,4-ethylenedioxythiophene) (PEDT)<sup>8</sup> (0.5% PEDT) that can be used to produce films that are very air-stable and transparent.

Another approach in making water-based processable ICPs was developed by Bjorklund and Liedberg<sup>9</sup> and intensively studied by Armes et al.,<sup>10</sup> employing water soluble polymers used as steric stabilizers for the emulsion polymerization of polypyrrole. The stabilizers become physically adsorbed on the polypyrrole particle surface and, like in an emulsion polymerization, very monodisperse particles are formed. If the polymerization of pyrrole is carried out in the presence of conventional latex particles, the conducting polymer may form a regular shell around those particles, as was shown by Yassar et al.<sup>11</sup> By choosing a suitable low  $T_g$  core latex, these polypyrrole-coated latex particles can exhibit very good film-forming properties at room temperature. DSM has commercialized a product based on this principle under the name Conquest. A second advantage of this approach is that the conducting polymer can be extremely diluted with a nonconducting polymer without loss of conductivity. This can be achieved by synthesizing a very thin conducting shell around the nonconducting latex core. We have prepared polypyrrole-coated poly(butyl methacrylate) latices for which the conductivity is almost independent of the conducting polymer content down to 1 wt %. The percolation threshold for these latices is as low as 0.25 wt % PPy.<sup>12</sup>

For some applications there is a need for transparent conducting coatings. Since the ICPs are conjugated, they absorb visible light and thus are strongly colored. Therefore, if one wants to make transparent films of these ICPs, a very thin coating or very strong dilution with other, transparent polymers is needed. As noted earlier, the core-

shell technique offers a very good opportunity to dilute the ICP strongly without loss of the conducting path. Hence, we have used such latices for the preparation of transparent conducting films.

For the formation of transparent films from aqueous latices, it is necessary that the sizes of the pores and voids in the film are much smaller than the wavelength of the visible light. This means for latex particles of the size that we use in this study (about 700 nm in diameter) that they have to deform considerably to fill the voids that are formed upon drying of the aqueous latex. Usually the film-formation process is described in terms of four distinct stages, separated by three transitions.<sup>13</sup> A schematic presentation of the film formation process is shown in Figure 1.

In stage 1 the latex particles are dispersed in the aqueous medium. The water evaporates at a rate close to that of pure water. At a particle volume fraction between 60% and 70%, the latex particles come into irreversible contact with each other (stage 2). Then there is a further, slower loss of water, accompanied by a deformation of the particles. Capillary forces tend to deform the particles, to fill all the voids left by water evaporation. A transparent film is formed at the end of the evaporation process if the voids between the latex particles after the evaporation of the water are small enough. If the resistance for particle deformation is too high (e.g., below the  $T_g$  of the polymer), voids will be left, thus leading to an opaque film. Increasing the temperature above the  $T_g$  of the polymer can allow the particles to deform further, thus leading to a transparent film. In this stage, stage 3, the particle contours are still present. To reach stage 4, the polymer chains of the individual latex particles interdiffuse across the particle interfaces. During this last step the film acquires its mechanical strength.

In the case of the conducting core-shell latex particles, the outer shell is formed by the rather rigid ICP. Therefore, the main difficulties in film formation are expected to appear in the last two

**Table I** Composition of the Reaction Mixture

Latex Code	PPy Content (wt %) <sup>a</sup>	Pyrrole ( $\mu$ l)	FeCl <sub>3</sub> ( $\mu$ l) <sup>b</sup>	H <sub>2</sub> O <sub>2</sub> ( $\mu$ l) <sup>c</sup>	Demineralized Water ( $\mu$ l)
1	1	46.0	187	74.8	4616
2	2	92.0	374	150	4309
3	4	184	748	299	3693

<sup>a</sup> Relative to PBMA.<sup>b</sup> Aqueous solution containing 0.29 wt % FeCl<sub>3</sub>.<sup>c</sup> Aqueous solution containing 35 wt % H<sub>2</sub>O<sub>2</sub>.

stages, where the surface of the latex particle has to deform and PBMA polymer chains have to diffuse through the rigid polypyrrole shell.

In a previous study, we showed that the speed of film formation of core-shell latex particles with a polypyrrole shell strongly depends on the annealing temperature.<sup>14</sup> Temperatures much higher than the  $T_g$  of PBMA are needed to establish film formation within reasonable time scales.<sup>12</sup> In the present work the effect of the thickness of the ICP shell on the film formation properties of the latex has been studied. We have studied the film formation of latices coated with 1, 2, and 4 wt % PPy. Based on the core diameter of 692 nm, this gives for the theoretical thickness of the polypyrrole shell 1.2, 2.3, and 4.6 nm, respectively. The techniques used to study the film formation of these conducting latices are transparency measurements, resistivity measurements, atomic force microscopy (AFM) surface flattening, and transmission electron microscopy (TEM) of ultrathin film sections.

## EXPERIMENTAL

### Poly(butyl methacrylate) Latex Synthesis

The core poly(butyl methacrylate) (PBMA) latex was synthesized in an emulsifier-free batch synthesis at 70°C. The butyl methacrylate (99%) monomer was purchased from Aldrich and was used without further purification. Ammonium persulfate (98+%, Aldrich) was used as initiator. The number-average diameter of the very monodisperse PBMA latex particles was determined using a Brookhaven Instruments BI-DCP Particle Size Analyzer, and found equal to  $692 \pm 18$  nm, with  $D_w/D_n = 1.001$ . The PBMA latex was dialyzed thoroughly in dialysis bags (MWCO 12,000–14,000 Da; Medicell International), until the conductivity of the water outside the dialysis

bag remained under 10  $\mu$ S/cm. The solid content of the PBMA latex after dialysis was 17.8 wt %.

### Polypyrrole Encapsulation Protocol

The conducting core-shell latex particles were synthesized using a method slightly different from that of Liu et al.<sup>15</sup> To 25 g of the PBMA latex dispersion (4.45 g of solid PBMA), 5.95 g of a 1 wt % aqueous solution of hydroxyethylcellulose (HEC; kindly donated by Hercules BV) was added and the system was allowed to stabilize for at least 30 min. Oxygen was removed by bubbling N<sub>2</sub> through the mixture. To this latex, different amounts of freshly distilled pyrrole (98%; Aldrich) were added depending on the desired PPy shell thickness. The exact amounts of pyrrole are given in Table I. The pH of the reaction mixtures was set to about 1 by the addition of 413  $\mu$ L of HCl (37%; Aldrich). To this, a certain amount of the Fenton's reagent [H<sub>2</sub>O<sub>2</sub> (35%; Aldrich) and FeCl<sub>3</sub> (97%; Aldrich)] was added as an oxidant. This oxidant is used because only a catalytic amount of the high valence Fe<sup>3+</sup> is introduced in the reaction mixture. The addition of high valence ions has a negative influence on the colloidal stability of the latex.<sup>15</sup> To keep the same concentration of the latex in all experiments, some demineralized water was added. All latices were thoroughly dialyzed before further use. The compositions of the reaction mixtures are given in Table I. The stability of the encapsulated latices was checked by means of dark-field microscopy. The amount of polypyrrole in the shell was not measured; only theoretical amounts are given in this study. We tried to determine the amount of polypyrrole on the latex particles using elemental analysis and XPS, but none of these methods showed reasonable precision to determine the (extremely small) amounts of polypyrrole.

### Dried Latex Electrical Resistivity Measurements

Resistivity was measured on pressed pellets of the filtered and vacuum-dried latex using a standard four-point method. To prevent the influence of contact resistance, gold electrodes were deposited on the pressed pellet.

### Film Transparency and Electrical Resistance Measurements

The effect of the concentration of the HEC stabilizer, postadded to pure PBMA latex dispersion, on the development of the transparency of the films was determined by measuring the transmittance at 600 nm using a Shimadzu UV-2101 PC UV-Vis scanning spectrophotometer. The latices were allowed to stabilize for 3 days under gentle stirring after the addition of the HEC. Films were cast from these latices on glass slides using a 150- $\mu\text{m}$  casting knife, resulting in dry films with a theoretical thickness of about 30  $\mu\text{m}$ . The wet films were partially covered to slow down the water evaporation and allowed to dry overnight in ambient atmosphere. Next, the samples were heated in an oven at 90°C. Samples were quickly cooled to room temperature.

The transparency and resistance of the conducting films were measured *in situ* using a home-built apparatus. Measurements were done on 2  $\times$  2-cm<sup>2</sup> glass slides on which were deposited four parallel gold lines, 12  $\times$  1 mm (length  $\times$  width) and spaced 4 mm apart. The films were deposited on the glass slides by dipcoating the glass slides in the conducting latex. The glass was corona-discharge pretreated, to improve the adhesion between the glass and the deposited film. The films were deposited at room temperature and allowed to dry for 1 h at high relative humidity to avoid fast drying. The glass slide was then placed in a sample holder in an air-flow oven. At this stage most of the water had evaporated, but the films were still turbid. The oven temperature was set at 25°C for the first 2 min of the measurement and then increased to 120°C, to increase the speed of film formation. The temperature of the air that was led into the oven reached 120°C in about 2 min. The temperature of the sample reached 120°C after only about 20 min because of the heat capacity of the different components in the oven.

The transparency of the film was measured according to the following procedure. Two photodiodes (Siemens, BPW 21,  $\lambda_{\text{max}}$  550 nm) were used, which first had been calibrated using the

same white-light source and a noncoated glass slide. One of the photodiodes, the reference, received the light directly from the light source, giving a signal S1. The other photodiode received the same light that had passed through a noncoated glass, giving a signal S2. The calibration factor is given by the ratio S1/S2. The transparency of the film was determined using the same procedure, only the glass slide was coated with the latex film according to the procedure just described. The transparency of the film is given by the ratio S2/S1, corrected by the calibration factor.

The resistance of the film was measured using the gold line electrodes according to the four-point method.

### AFM Surface Flattening Experiments

The flattening of the latex films during film formation was studied using an atomic force microscope according to a previously reported method.<sup>16</sup> Images were taken on an AutoProbe CP (Park Scientific Instruments, Sunnyvale, CA). The microscope was operated in the noncontact mode. The films used for the flattening experiments were prepared by pouring a few drops of the latex onto glass slides and allowing the latex to dry completely at room temperature. The glass slides were partly covered to slow down evaporation and thus facilitate the ordering of the latex particles.<sup>17</sup> Films of about 1-mm thickness were thus obtained. A small part of the dried film was then glued to an AFM sample holder using adhesive tape. The first image was taken without any heat treatment (nascent film) less than 1 day after drying. Film formation was allowed to proceed at 120°C in an oven for various periods of time. The samples were removed from the oven and quickly cooled to room temperature (i.e., below the  $T_g$  of PBMA). From each sample a 10  $\times$  10- $\mu\text{m}^2$  image was taken at four different spots. From each image, the  $R_{\text{rms}}$  surface roughness was determined on two different 5  $\times$  5- $\mu\text{m}^2$  spots. The listed values for the  $R_{\text{rms}}$  surface roughness are the average of these eight measurements. To eliminate long-range imperfections, third-order line-flattening processing was performed on all images.

### Ultrastructural TEM Study of Void Closure

The films for transmission electron microscopy were prepared by a method similar to the one

**Table II Conductivity and Stability of the Conducting Latexes**

Latex Code	Pellet Conductivity (S/cm)	Latex Stability
1	0.16	Stable
2	0.22	Stable
3	0.53	Slightly flocculated

used in the AFM surface flattening experiments. The films were divided into different parts. One part of the film was analyzed without further heat treatment. Other parts of the same films were placed in an oven at 120°C for different annealing times. Ultrathin sections of about 80-nm thickness were cut using a Reichert Jung FC4D microtome at a setting temperature of -120°C and deposited on 200-mesh nickel grids coated with a formvar support film. The sections were imaged in a Philips CM 100 transmission electron microscope operating at a 60-kV acceleration voltage without additional contrasting.

## RESULTS AND DISCUSSION

### Properties of Latexes and Films

The pellet conductivity and the stability of the latexes obtained from the *in situ* polymerization of pyrrole in the presence of the PBMA latex are given in Table II.

The results for the pellet conductivities are comparable to those reported previously.<sup>10</sup> The TEM and AFM results, discussed below, demonstrated that the PPy forms a smooth shell around the PBMA core, even for sample 3, whose film-forming properties can therefore be compared to those of the other two latexes. To make 4 wt % PPy latexes with better colloidal stability, the amount of HEC can be increased; however, this has a negative influence on the transparency and rate of film formation of latexes, as can be seen from Figure 2. The HEC concentrations are given relative to the solid latex content.

PBMA latex films with amounts of HEC higher than 1.3 wt % appear cloudy, not clear. Above this concentration of HEC, in our estimation, the amount of "free" HEC in the water phase is so high that HEC clusters are formed in the film upon evaporation of the water. Because of a difference in refractive index between these clusters

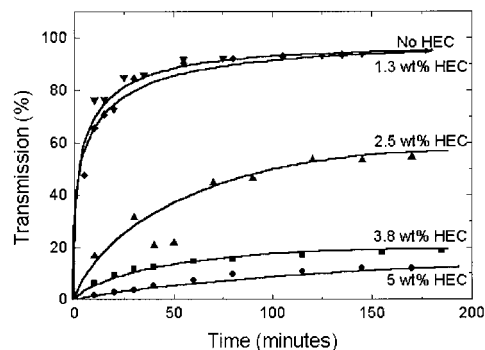


**Figure 2** Influence of the amount of HEC on the transparency and rate of film formation at 90°C of an approximately 30- $\mu$ m-thick film of the pure PBMA (core) latex measured at a wavelength of 600 nm.

and the matrix film, the clusters will scatter light and therefore limit the maximum film transparency that can be obtained.

In Figure 3 a typical plot of the development of

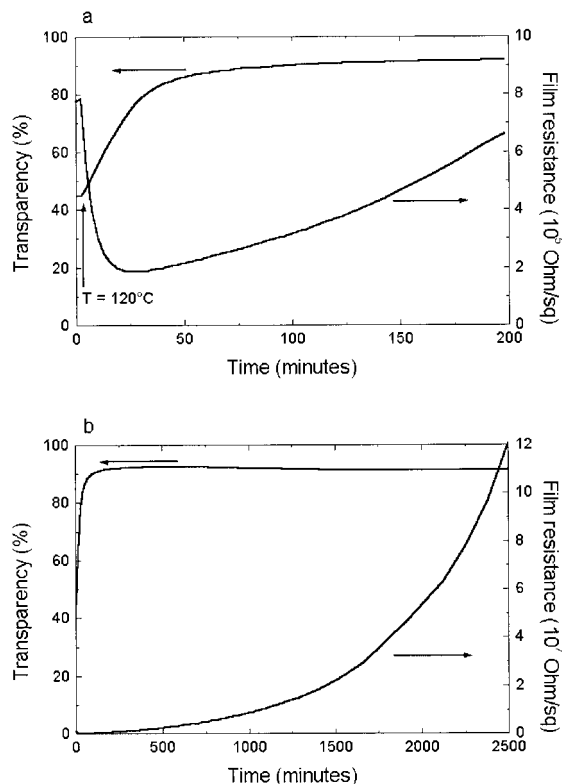


**Figure 3** Development of transparency and resistance of a 1 wt % PPy latex film at 120°C. Measurements are done on the same sample at the same time in the resistance/transparency cell: (a) initial changes; (b) long-time behavior.

the transparency and resistance of a 1 wt % PPy latex film is shown.

The resistance of the conducting latex film strongly decreases when, after 2 min, the temperature is increased from 25°C to 120°C. At 25°C the resistance of the film is about 800 k $\Omega/\square$ . At the minimum observed in the resistance curve after about 25 min, the film resistance is less than 200 k $\Omega/\square$ , or less than 25% of the initial resistance at 25°C. Two effects explain the decrease of the film resistance upon heating. First, the conductivity of PPy increases with mild heating.<sup>18,19</sup> Furthermore, increasing the temperature allows the latex particles to deform and close the voids in the film, which increases the contact area between the conducting shells of different particles. Thus hopping of electrons between the different polypyrrole shells is facilitated.

After about 25 min the resistance increases until after about 2500 min the resistance exceeds 100 M $\Omega/\square$  and the film is no longer called anti-static. The increase of the resistance at 120°C in air can be attributed to the thermal degradation of polypyrrole. The major contribution comes from the reaction of the polypyrrole chain with oxygen from air.<sup>20</sup> A second kind of degradation taking place is the loss of the Cl<sup>-</sup> counteranion, involving HCl volatilization from the films.<sup>21</sup> We previously showed that, in the case of these conducting core-shell latices, both mechanisms play a role.<sup>22</sup>

The process of latex film formation is shown in Figure 1. If a latex film is dried below the  $T_g$  of the polymer, the deformation of the particles is seriously hindered and the process will stop at stage 2. Voids will remain present in the film. If the size of these voids is of the same order of magnitude as the wavelength of visible light, these voids will scatter the light, thus giving the film an opaque appearance.

In our case the outer layer of the latex particles is formed by polypyrrole. This polymer is infusible and will always be in its glassy state at the temperatures used to form the film, even at the annealing temperature of 120°C. The implications of this are discussed below. The core of the latex consists of PBMA. The  $T_g$  of this polymer is about 35°C (i.e., above room temperature). Therefore, we can expect a film formed at room temperature to be opaque. Indeed, this has been observed and is demonstrated in Figure 3, which shows that the transparency of the film dried at room temperature is only about 50%. Upon heating this film to 120°C, far above the  $T_g$  of PBMA, the particles deform and fill the voids. This leads to an increase

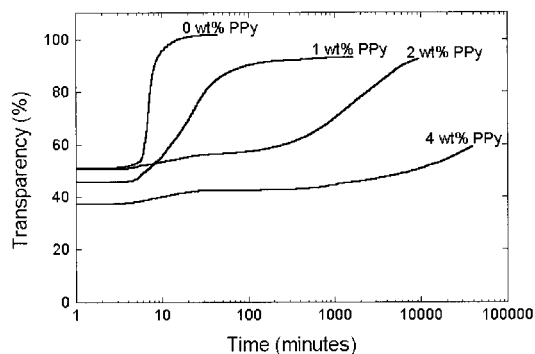


**Figure 4** Comparison of the development of the transparency at 120°C of latices with different PPy shell thickness.

of the film transparency. The final transparency of the film is about 92%. The remaining 8% of the light is either absorbed, scattered by voids that are still present, or reflected by the latex film surface.<sup>23</sup>

#### Influence of Shell Thickness on Film Transparency

We measured the development of the transparency of the film as a function of time at 120°C. In Figure 4 the development of the transparency for different thicknesses of the conducting polypyrrole shell is shown.

The transparency before heating of the latices with both 1 and 2 wt % PPy and of those without polypyrrole is comparable (i.e., around 50%). The transparency of the 4 wt % PPy latex film is somewhat lower (i.e., about 37%). This might be explained by the fact that the 4 wt % PPy latex is less colloiddally stable than the other latices and forms small aggregates in the dispersion. Filtration to remove these aggregates does not help since aggregates are formed again upon evaporation of water, which gives a poorer stacking of the latex particles. Therefore more and larger voids will be present in sample film 3 and more light will be scattered.

The development of the transparency strongly depends on the thickness of the polypyrrole shell. Although the thickness of the shell is very small compared to the diameter of the core, it is the determining factor for the development of the transparency. The final transparency of the films containing 1 and 2 wt % polypyrrole, however, seems to be fairly independent of the PPy content. This suggests that the absorption of light by polypyrrole is not the determining factor. The voids between the particles have disappeared or, at

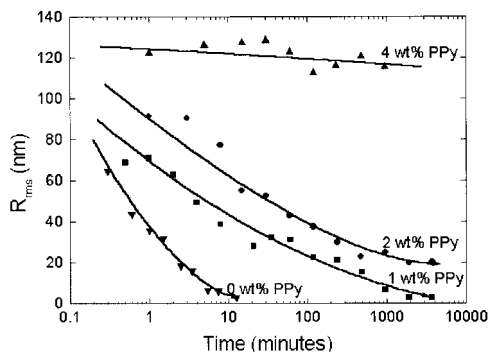


**Figure 5** Development of the  $R_{\text{rms}}$  roughness at 120°C of latices with different PPy contents.

least, reduced in size considerably (see section on ultrastructural TEM study, below). Since the size of the latex particles used in this study is relatively large, light can be scattered by voids between the particles, even if they are relatively small.<sup>24</sup> It is clear from the TEM results, however, that the eventually residual voids must be extremely small in this case. The scattering of visible light by such small voids is very low.<sup>22</sup> Therefore we postulate that reflection of light is the main factor determining the final film transparency. Additional evidence in favor of this hypothesis is the fact that the final transparency of the pure PBMA film is clearly higher. In this case the refractive index of the film surface is lower and only PBMA–air boundaries are present, giving rise to a lower degree of reflection. Another factor that might influence the reflection, and thus the development of the film transparency, is the roughness of the film surface, the development of which we investigated using AFM.

#### Atomic Force Microscopy Study of Surface Flattening during Film Formation

We investigated the flattening of the latex particles upon heating the films at 120°C. In Figure 5 the decrease of the  $R_{\text{rms}}$  surface roughness at 120°C is plotted for the different PPy contents. The  $R_{\text{rms}}$  roughness is given by the standard deviation of the AFM height data, determined using the standard definition:

$$R_{\text{rms}} = \left[ \frac{\sum_{n=1}^N (z_n - \bar{z})^2}{N - 1} \right]^{1/2}$$

where  $\bar{z}$  = mean  $z$  height.

The PBMA latex without a polypyrrole shell flattens very fast at 120°C; after 10 min the surface is almost completely flat, which is as expected since the  $T_g$  of poly(butyl methacrylate) is about 35°C. Even a very thin polypyrrole shell of about 1.2-nm thickness remarkably reduces the speed of flattening. For the 1 wt % PPy latex it takes 30 h at 120°C to flatten as much as the pure PBMA latex in 10 min at 120°C. The decrease in surface roughness of the 2 wt % PPy sample is much slower than that of the 1 wt % PPy latex, although it shows a similar behavior. The sample with 4 wt % PPy, shell thickness about 4.6 nm, shows a different behavior. First, the initial surface roughness is much higher than that for the other samples. As stated earlier, in our opinion this can be attributed to the lower stability and, therefore, poorer stacking of the latex particles in the sample. This difference in stacking was demonstrated by the AFM images. A second difference is that the flattening process is much slower in the 4 wt % PPy sample than it is in the other samples. The polypyrrole shell very severely hinders the deformation of the latex particles.

#### Ultrastructural TEM Study of Void Closure during Film Formation

The deformation of the latex particles during film formation was also studied by transmission electron microscopy on ultrathin sections of the dried latices. Because of the highly conjugated system, the polypyrrole shell absorbs many more electrons than does the PBMA core. Therefore the contours of the individual latex particles and the polypyrrole shells are clearly visible without additional contrasting. The pictures shown in Figure 6 are pure sections of the dried latices, without any further treatment.

In the samples without any heat treatment, voids between the latex particles are clearly visible, especially in the samples with relatively thick PPy shells. Light is scattered by these voids, leading to an opaque film appearance. There are more and larger voids in the sample with 4 wt % PPy than in the 2 wt % PPy samples; the number and size of the voids in the 1 wt % PPy sample are even lower. The voids in the 1 and 2 wt % PPy samples seem to have disappeared after 19 min and 20 h at 120°C, respectively, whereas the transparency of thin films increased to only about 70% after such a heat treatment (see Fig. 4). These effects can be attributed to the deformation of the particles by capillary forces, whose magni-

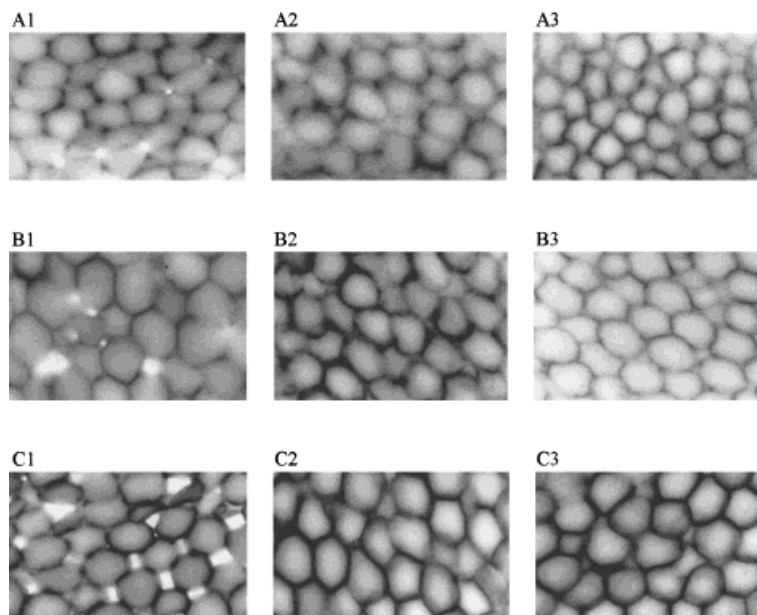


**Figure 6** Transmission electron micrographs taken from about 80-nm ultrathin sections after different annealing times at 120°C. (A1) 1 wt % PPy, no heat treatment; (A2) 1 wt % PPy, 19 min; (A3) 1 wt % PPy, 4 days; (B1) 2 wt % PPy, no heat treatment; (B2) 2 wt % PPy, 20 h; (B3) 2 wt % PPy, 4 days; (C1) 4 wt % PPy, no heat treatment; (C2) 4 wt % PPy, 28 days; (C3) 4 wt % PPy, 74 days.

tude is of the same order as the force necessary to deform particles close to the  $T_g$ .<sup>25</sup> In our case, the drying of the latex droplets used for the TEM study proceeds much slower than that of the thin ( $\pm 2 \mu\text{m}$ ) films used for the transparency study, leaving less time in the latter case to creep and deform. We tried to slow down the water evaporation from the thin films as much as possible by drying the films over a water surface in about 1 h but, even then, the drying of the thin film is much faster than the drying of the latex droplets. Therefore, in the latter, the deformation forces have more time to operate and the particles are deformed more.<sup>26</sup> In the case of the 4 wt % PPy sample, the resistance against deformation is so high that the capillary forces have less influence on the deformation of the particles. Furthermore, because of the poorer colloidal stability of latex sample 3, larger voids will be present in the latex film upon drying. Hence the micrographs of the ultrathin sections support the conclusions drawn from the transparency measurements, taking into account that the time necessary to close the voids between the particles strongly depends on the drying conditions. Moreover, an extra support for this conclusion is the fact that the initial transparency of the latex film strongly depends on the evaporation rate of water. If the evaporation rate

is increased by drying the films in an air stream, the initial film transparency is about 25% instead of 45%. The final transparency after heating such films to 120°C, however, is independent of the initial transparency.

#### Influence of Shell Thickness on Electrical Resistance

As shown in Table II, the resistivity of pressed pellets of dried powders of these latices with different shell thickness is of the same order of magnitude. The development of the resistance with time of these latices at 120°C is shown in Figure 7.

The initial film resistance is in the same order of magnitude for each shell thickness, as was expected, based on the pressed pellet conductivities. The variations in the absolute value are most likely the result of variations in the film thickness. After increasing the temperature to 120°C, the resistance of all the films decreases and the minimum resistance is reached after about 20 min. Thereafter the resistance of the films increases, although the increase is much slower in the case of the 1 wt % PPy film than in the two other cases. A possible explanation for this difference might be that the closure of the voids between the particles of the film with 1 wt % PPy is



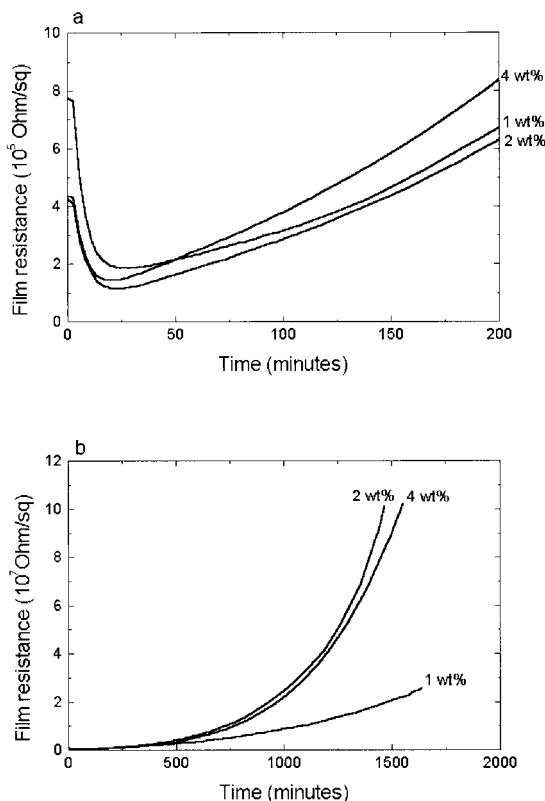


**Figure 7** Comparison of the development of the film resistance at 120°C of latices with different shell thickness: (a) initial change; (b) long-time behavior.

much faster than that with the other two latices. It is known that the conductivity of films is more stable than that of powders<sup>19</sup> and it is possible that the films based on the 2 and 4 wt % PPy latices behave more like powders in this respect because voids remain in these films for a long time. The denser structure of the film based on the 1 wt % PPy latex might hinder the loss of the counteranion, the entrance of oxygen in the film, and the overoxidation of the polypyrrole chain that leads to an increase in the film resistance. More work must be done, to understand the part played by the existence of voids in the film on the resistance of the film.

## CONCLUSIONS

Highly transparent (>90%), antistatic polymer films were prepared from conducting core-shell latices by heating the latex far above the  $T_g$  of the core material. The latex particles are composed of a core (about 700 nm in diameter) of poly(butyl

methacrylate) and a thin shell of polypyrrole. The amount of polypyrrole was varied between 1 and 4 wt %, giving a PPy shell thickness between 1.2 and 4.6 nm. The influence of the PPy shell thickness on the latex film-formation process was studied using transparency measurements, atomic force microscopy surface flattening measurements, and transmission electron microscopy on ultrathin sections of the latex film. All results merge to the conclusion that the speed of film formation strongly depends on the thickness of the polypyrrole shell. Furthermore, it was shown that the final transparency of the latex film seems to be independent of the shell thickness. This indicates that light absorption by the polypyrrole is not the determining factor for the film transparency. Transmission electron microscopy on ultrathin sections of the latex films showed that no voids, or possibly only extremely small voids, are present in the film long before maximum film transparency is reached. This suggests that reflection of light plays an important role in the development of the film transparency. A correlation has been found between the development of the transparency and the film surface roughness. As the flattening of the film increases, the reflection of light at the film surface probably decreases, which may contribute to the increase of the film transparency. More work must be done to determine the role of reflection on the film transparency.

The film conductivity only slightly depends on the amount of polypyrrole; the stability of the conductivity is even better for the latex with 1 wt % PPy. The film resistance initially decreases upon increasing the temperature because of the semiconductor-like behavior of ICPs and the densification of the film. After about 20 min at 120°C the resistance starts to increase as a result of the degradation of the ICP. The resistance of the films exceeds the antistatic limit after about 1–2 days at 120°C in air.

The best results have been obtained for a PBMA latex with a 1 wt % polypyrrole shell. This latex gives the best combination of a conductivity in the antistatic region and a relatively fast film formation.

The authors thank Dr. Paul van Hutten (University of Groningen, Polymer Chemistry) for valuable discussion. F.H. appreciates the financial support provided by the Senter IOP Surface Technology (IOT 95001 B), especially the extra financial support for a stay at the Institut Charles Sadron.

## REFERENCES

1. Angelopoulos, M.; Asturias, G. E.; Ermer, S. P.; Ray, A.; Scherr, E. M.; MacDiarmid, A. G. *Mol Cryst Liq Cryst Sci Technol* 1988, 160, 151.
2. Cao, Y.; Smith, P.; Heeger, A. J. *Synth Met* 1992, 48, 91.
3. Hopkins, A. R.; Rasmussen, P. G.; Basheer, R. A. *Macromolecules* 1996, 29, 7838.
4. Harlev, E.; Gulakhmedova, T.; Rubinovich, I.; Aizenshtein, G. *Adv Mater* 1996, 8, 994.
5. Andreatta, A.; Cao, Y.; Chiang, J.-C.; Smith, P.; Heeger, A. J. *Synth Met* 1988, 26, 383.
6. Cao, Y.; Smith, P.; Heeger, A. J. *Synth Met* 1989, 32, 263.
7. Lee, J. Y.; Kim, D. Y.; Kim, C. Y. *Synth Met* 1995, 74, 103.
8. Jonas, F.; Kraft, W.; Muys, B. *Macromol Symp* 1995, 100, 169.
9. Bjorklund, R. B.; Liedberg, B. *J Chem Soc Chem Commun* 1986, 1293.
10. Armes, S. P.; Vincent, B. *J Chem Soc Chem Commun* 1987, 288; Armes, S. P.; Miller, J. F.; Vincent, B. *J Colloid Interface Sci* 1987, 118, 410.
11. Yassar, A.; Roncali, J.; Garnier, F. *Polym Commun* 1987, 28, 103.
12. Huijs, F. M.; Vercauteren, F. F.; de Ruiter, B.; Kalicharan, D.; Hadziioannou, G. *Synth Met* 1999, 102, 1151.
13. Keddie, J. L.; Meredith, P.; Jones, R. A. L.; Donald, A. M. *Macromolecules* 1995, 28, 2673.
14. Huijs, F. M.; Lang, J. *Colloid Polym Sci* 2000, 278, 746.
15. Liu, C.-F.; Maruyama, T.; Yamamoto, T. *Polym J* 1993, 25, 363.
16. Juhué, D.; Lang, J. *Colloids Surf A* 1994, 87, 177.
17. Micheletto, R.; Fukuda, H.; Ohtsu, M. *Langmuir* 1995, 11, 3333.
18. Ansari, R.; Wallace, G. G. *Polymer* 1994, 35, 2372.
19. Li, Y.; Imaeda, K.; Inokuchi, H. *Polym J* 1996, 28, 559.
20. Thiéblemont, J. C.; Brun, A.; Marty, J.; Planche, M. F.; Calo, P. *Polymer* 1995, 36, 1605.
21. Thiéblemont, J. C.; Planche, M. F.; Petrescu, C.; Bouvier, J. M.; Bidan, G. *Synth Met* 1993, 59, 81.
22. Huijs, F. M.; Vercauteren, F. F.; de Ruiter, B.; Hadziioannou, G. in *Conductive Coatings and Compounds, Proceedings of the Paint Research Association, Middlesex, U.K., June 21–22, 1999; 1999*.
23. van Krevelen, D.W. in *Properties of Polymers*, 3rd ed.; Elsevier Science B.V.: Amsterdam, 1997; Chapter 10.
24. van Tent, A. Ph.D. Thesis, Technical University Delft, 1992; Chapter 4.
25. Visscher, M.; Laven, J.; van der Linden, R. *Prog Org Coat* 1997, 31, 311.
26. Sperry, P. R.; Snyder, B. S.; O'Dowd, M. L.; Lesko, P. M. *Langmuir* 1994, 10, 2619.